

Propagating magnetohydrodynamics waves in coronal loops

BY I. DE MOORTEL*

*School of Mathematics and Statistics, University of St Andrews, North Haugh,
St Andrews KY16 9SS, UK*

High cadence Transition Region and Coronal Explorer (TRACE) observations show that outward propagating intensity disturbances are a common feature in large, quiescent coronal loops, close to active regions. An overview is given of measured parameters of such longitudinal oscillations in coronal loops. The observed oscillations are interpreted as propagating slow magnetoacoustic waves and are unlikely to be flare-driven. A strong correlation, between the loop position and the periodicity of the oscillations, provides evidence that the underlying oscillations can propagate through the transition region and into the corona. Both a one- and a two-dimensional theoretical model of slow magnetoacoustic waves are presented to explain the very short observed damping lengths. The results of these numerical simulations are compared with the TRACE observations and show that a combination of the area divergence and thermal conduction agrees well with the observed amplitude decay. Additionally, the usefulness of wavelet analysis is discussed, showing that care has to be taken when interpreting the results of wavelet analysis, and a good knowledge of all possible factors that might influence or distort the results is a necessity.

Keywords: Sun; corona; oscillations; waves

1. Introduction

The detection of oscillations in coronal loops is crucial in order to determine the presence and relevance of coronal heating mechanisms based on the dissipation of magnetohydrodynamics (MHD) waves. Through ‘coronal seismology’, detecting oscillations in coronal loops can also improve existing estimates of coronal properties and dissipation coefficients, vital information for both numerical and theoretical coronal heating models. Although the theoretical possibility of coronal seismology was suggested quite a while ago (Roberts *et al.* 1984), it is only now that spaced-based observations by satellites such as Solar and Heliospheric Observatory (SOHO) and Transition Region and Coronal Explorer (TRACE) enable us to truly develop this idea. Indeed, slowly but surely, observational examples of all the different types of MHD waves are being discovered. There are now numerous reports on the detection of propagating and

*ineke@mcs.st-and.ac.uk

One contribution of 20 to a Discussion Meeting Issue ‘MHD waves and oscillations in the solar plasma’.

standing slow waves, as well as fast waves, mainly in coronal loops, but also in other structures such as coronal plumes and prominences. In this paper, we will concentrate on periodic intensity disturbances that are observed to propagate along coronal loops. For a more in-depth review of observed oscillations in the solar corona, as well as the development of coronal seismology, we refer the reader to De Moortel (2005) and Nakariakov & Verwichte (2005).

2. Wavelet analysis

During recent years, wavelet analysis (Torrence & Compo 1998) has become an increasingly popular method to analyse observed (solar) oscillations. As most of the observed time-series are non-stationary, wavelet analysis is well suited, providing the time localization of the various frequency components.

Let us assume a time-series x_n of N observations with cadence δt . The continuous wavelet transform is then defined as the convolution of x_n with a mother wavelet $\psi(\eta)$ (assumed to be normalized). For $\eta = (n' - n)\delta t/s$, we have

$$W_n(s) = \sum_{n'=0}^{N-1} x_{n'} \sqrt{\frac{\delta t}{s}} \psi^* \left[\frac{(n' - n)\delta t}{s} \right], \quad (2.1)$$

where s is the wavelet scale and n governs the translation of the analysing wavelet in time. By varying s and n , a picture of any features in the time-series as a function of the scale s and the localized time index n can be constructed. The wavelet transform suffers from edge effects at both ends of the time-series, resulting in a cone of influence (COI); portions of the transform outside the area formed by the time axis and the COI are subject to these edge effects and, hence, unreliable.

The choice of the appropriate mother wavelet depends on the nature of the signal and on the type of information to be extracted from the signal. We will here only consider two different mother wavelets, namely the Morlet wavelet,

$$\psi(\eta) = \pi^{-1/4} e^{ik\eta} e^{-\eta^2/2}, \quad (2.2)$$

and the Paul wavelet,

$$\psi(\eta) = \frac{2^k i^k k!}{\sqrt{\pi(2\pi)!}} (1 - i\eta)^{-(k+1)}. \quad (2.3)$$

The value of the wavelet parameter, k , controls the number of oscillations present in the mother wavelet and, hence, will strongly influence the frequency and time resolution of the corresponding wavelet transform.

De Moortel *et al.* (2004a) demonstrated both the potential and the difficulties of wavelet analysis. Using basic harmonic oscillations to examine the robustness of wavelet analysis, a significant difference was found in the time and frequency resolution, depending on both the mother wavelet and the value of the wavelet parameter. The best frequency resolution is obtained with the Morlet wavelet and a large k , whereas the best time resolution is achieved with the Paul wavelet, and a small value of k . For both mother wavelets, a better time resolution is obtained for smaller values of the wavelet parameter, whereas the frequency

resolution improves for larger values. Additionally, the time resolution of the Paul wavelet, for any value of the wavelet parameter, was found to be better than the Morlet wavelet. Owing to the fact that the basic Paul wavelet is much more confined (in time) than the Morlet wavelet, the transform is less affected by the edge effects. Hence, the COI associated with the Paul wavelet extends much higher, so that larger parts of the wavelet power can be considered reliable. This could be especially important when analysing signals of short duration, or periodicities that are relatively long, compared with the length of the time-series.

3. Observations of propagating slow waves

The first detection of propagating slow waves was made in Ultraviolet Coronagraph Spectrometer (UVCS)/SOHO observations of coronal holes, high above the limb by Ofman *et al.* (1997, 2000*a*). Similar compressive disturbances, with amplitudes of the order of 10–20%, and periods of 10–15 min, were detected by DeForest & Gurman (1998), analysing Extreme-ultraviolet Imaging Telescope (EIT)/SOHO observations of polar plumes. Ofman *et al.* (1999, 2000*b*) identified the observed compressive disturbances as propagating, slow magnetoacoustic waves, damped by compressive viscosity. Soon afterward, similar quasi-periodic disturbances were observed in coronal loops by TRACE (Nightingale *et al.* 1999; Schrijver *et al.* 1999; De Moortel *et al.* 2000) and EIT/SOHO (Berghmans & Clette 1999).

An overview of observed properties of such propagating intensity perturbations was given by De Moortel *et al.* (2002*a,b*) and we here summarize briefly the main results. The disturbances are detected, generally, in the lower parts of large, quiescent coronal loops (see figure 1 for an example), situated either at the edge of active regions or above sunspot umbras and they appear to be a widespread phenomena. The time-variable behaviour of the loops is extracted by creating a running difference of the intensity along the loop. An example of such a running difference image is shown in figure 1*b*. The clear, diagonal ridges of higher (bright) and lower (dark) intensity indicate that a disturbance is travelling along the coronal structure. The propagation speed was determined from the slope of the diagonal bands in the running-difference images. Note that, because of projection effects, the quoted values are only a lower limit for the true propagation speed. For this particular example, the propagation speed was estimated to be in the range of 75–125 km s⁻¹. In all the observed cases, only propagation away from the loop footpoints is observed, with an average speed (at ~ 1 MK) of the order of $v \approx 122 \pm 43$ km s⁻¹. The small-amplitude intensity variations only amount to $4.1 \pm 1.5\%$ of the background loop intensity. As an example, the time-series of the intensity at about 10 Mm along the loop marked in figure 1 is shown in figure 2*a*. The dot-dashed line represents a linear fit, which was subtracted from the data, prior to the wavelet analysis, to account for any global brightness changes in the loop structure.

Figure 2*b* shows the corresponding wavelet transform of the intensity at 10 Mm along the loops. The shaded contours correspond to the Morlet wavelet transform, the line contours to the Paul transform. At this position, the periods found inside the COI, and above the confidence level, cover a range of 195–350 s, with the maximum power situated at around 255 s. At this position the

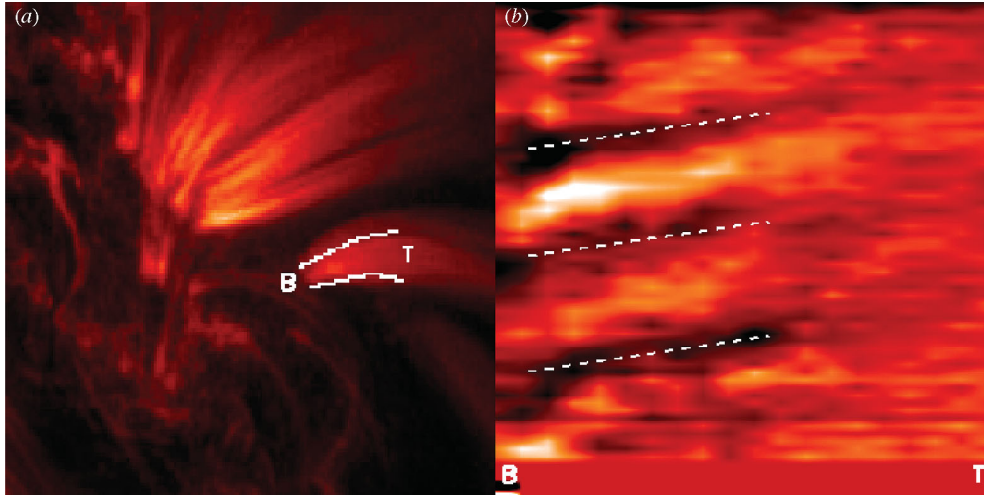


Figure 1. (a) An example (TRACE 171 Å—7 April 2000, 1242 UT) of a coronal loop footpoint supporting an oscillatory signal and (b) the running difference, between the intensity time-series, in which the propagating intensity disturbances are seen as bright and dark, diagonal bands.

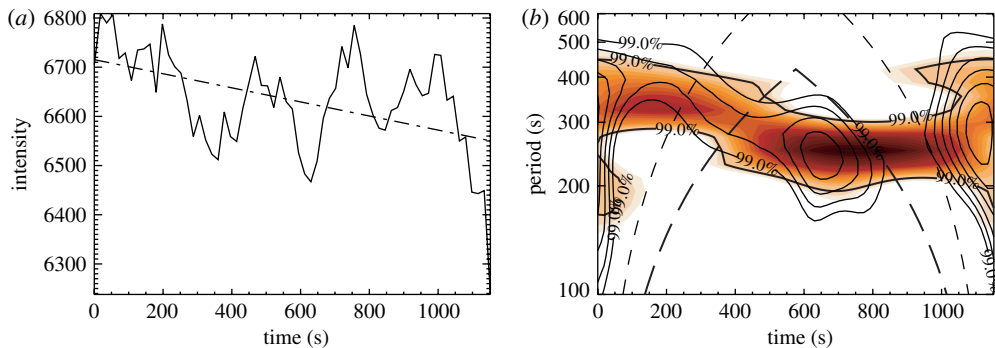


Figure 2. (a) The intensity oscillation at about 10 Mm along the loop, as a function of time. (b) Corresponding wavelet transform, where the thick lines (and filled contours) are obtained using the Morlet wavelet and the thin lines using the Paul wavelet. The long dashed lines correspond to the respective cones of influence.

maximum periodicity picked up by the respective wavelets is very similar (*ca* 250 s), although it occurs slightly later in time in the Morlet transform. The Paul transform extends less far in time, but is spread out in frequency, in accordance with our earlier results (§2). Note also that the COI of the Paul transform indeed extends much higher than the COI of the Morlet transform.

Including all 38 examples of De Moortel *et al.* (2000), periods of the order of 282 ± 93 s are found, but De Moortel *et al.* (2002c) showed a distinct separation between those loops situated above sunspots ($P \sim 172 \pm 32$ s) and those above non-sunspot or plage regions ($P \sim 321 \pm 74$ s). Given the small amplitudes, the energy flux in the observed disturbances is estimated to only be 342 ± 126 ergs $\text{cm}^{-2} \text{s}^{-1}$. This is several orders of magnitude below the energy necessary to maintain the temperature of quiescent coronal loops, which require *ca* 10^6 ergs $\text{cm}^{-2} \text{s}^{-1}$. The propagating disturbances were typically only detected

Table 1. Overview of the periodicities and propagation speeds of propagating slow MHD waves detected in coronal loops.

references	period (s)	speed (km s ⁻¹)	wavelength
Nightingale <i>et al.</i> (1999)	—	130–190	171 and 195
Schrijver <i>et al.</i> (1999)	300	70–100	195
Berghmans & Clette (1999)	~ 600	75–200	195
De Moortel <i>et al.</i> (2000)	180–420	70–165	171
Robbrecht <i>et al.</i> (2001)	—	65–150	171 and 195
Berghmans <i>et al.</i> (2001)	—	~ 300	SXT
De Moortel <i>et al.</i> (2002a)	(282 ± 93)	122 ± 43	171
De Moortel <i>et al.</i> (2002c)	172 ± 32 (sunsp.) 321 ± 74 (plage)	—	171
King <i>et al.</i> (2003)	120–180 and 300–480	25–40	171 and 195

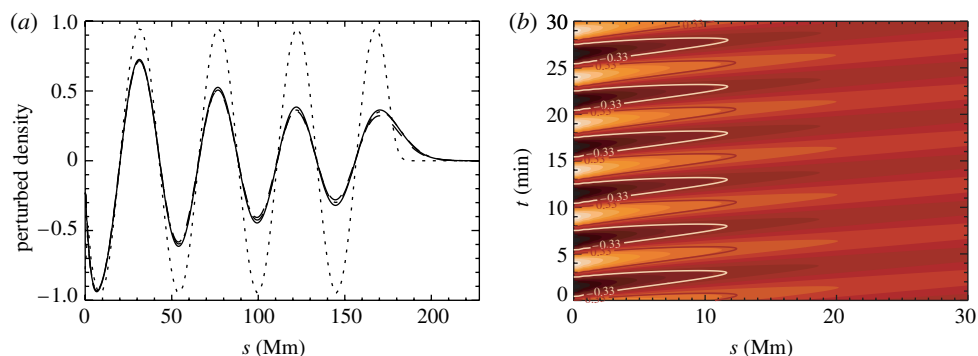


Figure 3. (a) A cross-section of the perturbed density (solid line) as a function of height, for which $d=0.025$ and $\epsilon=r=0$. The dotted line shows the ideal result, $d=0$. The dot-dashed line corresponds to $d=0.025$, $\epsilon=0.00086$ and $r=0$, whereas the dashed line corresponds to $d=0.025$, $\epsilon=0$ and $r=0.06$. (b) Contour plot of the density perturbations as a function of height and time, for which $d=0.025$, $r_0=1.6$ Mm and $\theta=7.1^\circ$.

in the first 2.9–23.2 Mm along the loop. However, this detection length is affected by the line-of-sight effects and additionally only indicates where the intensity changes vanish into the data noise, i.e. below the 99.0% confidence level.

An overview of the periods and propagation speeds found by various authors is given in table 1. In all cases, the propagation speed is of the order of the coronal sound speed, at the corresponding temperature, and generally, no significant acceleration or deceleration is observed. Additionally, the oscillations are observed as intensity oscillations and hence are likely to be compressive disturbances. The combination of these two facts leads to the interpretation of the observed oscillations as propagating, slow magnetoacoustic waves.

4. Theoretical modelling of propagating slow waves

Based on the above observations, Nakariakov *et al.* (2000) presented a model, in terms of slow magnetoacoustic waves, and concluded that the main factors

influencing the wave evolution are dissipation and stratification. The model was further developed by Tsiklauri & Nakariakov (2001), who incorporated the effect of a non-zero inclination angle and a semi-circular loop offset. These latter authors also show that, although the observed energy flux is insufficient, a wide-spectrum of similar slow magnetoacoustic waves could provide a sufficient rate of heat deposition to heat the coronal loops.

To study the dissipation in more detail, De Moortel & Hood (2003, 2004) investigated the properties of slow MHD waves travelling in an isothermal medium, including thermal conduction, compressive viscosity and optically thin radiation, as well as the effects of gravitational stratification and a diverging magnetic field geometry. The dissipative mechanisms are governed by three dimensionless parameters, namely a thermal ratio, d (ratio of the sound travel time and the thermal conduction time-scale), a viscosity coefficient, ϵ (effectively the inverse of the Reynolds number) and the radiation ratio, r (ratio of the sound speed and the radiation time-scale). For the exact definitions of these parameters, we refer the reader to De Moortel & Hood (2003, 2004). Using typical coronal values and a time-scale $\tau=300$ s yields a thermal ratio $d=0.025$, a viscosity coefficient $\epsilon=0.00086$ and a radiation ratio $r=0.06$.

Figure 3a shows the density perturbations as a function of height at a constant time, driven with an infinite harmonic wavetrain and without gravitational stratification or area divergence. The solid line was obtained including only thermal conduction, the dot-dashed line represents the effects of thermal conduction and compressive viscosity, whereas the dashed line shows damping due to thermal conduction and optically thin radiation. The dotted line shows the result in an ideal plasma. Clearly, thermal conduction (solid line) causes an amplitude decline of the relative density and, under the given coronal conditions (i.e. $T \approx 10^6$ K), the additional effect of either (compressive) viscosity or radiation appears negligible. Unfortunately, increasing the thermal conductivity does not result in the required damping rate to match with observations, as there is a minimum damping length that can be obtained by thermal conduction alone (De Moortel & Hood 2003). In the limit of large d , the perturbations are only weakly damped and additionally, travel at the slower, isothermal sound speed.

Subsequently, De Moortel & Hood (2004) studied the effect of area divergence, using a coronal loop cross-sectional area

$$A(s) = \pi(r_0 + s \tan(\theta))^2, \quad (4.1)$$

where $r_0=1.6 \pm 0.37$ Mm is the average observed radius at the base of the loop and $\theta=7.1 \pm 3.8^\circ$ is the average observed expansion angle for the 38 examples considered by De Moortel *et al.* (2002a).

Including area divergence, gravitational stratification (scale height $H \approx 50$ Mm) and thermal conduction ($d=0.025$), figure 3b shows a contour plot of the density perturbations. In this case, the perturbations would only have been detected (solid contours) in the first 10–20 Mm along the loop, which is in good agreement with the observed values. Using numerical simulations, the model was further developed by Klimchuk *et al.* (2004), who investigated the nonlinear damping by thermal conduction, in a non-isothermal loop. They find that, unlike the density perturbations, the intensity perturbations do not depend directly on the area variation. However, in the non-isothermal atmosphere, the intensity

variations decrease very quickly due to a combination of damping by thermal conduction and the effect of the instrument response function (TRACE 171 Å) and again, good agreement with observed values is obtained. A similar conclusion was reached by [Ofman & Wang \(2002\)](#), who demonstrated that the rapid damping of standing slow waves, observed in hot coronal loops (greater than 6 MK), could be explained in terms of ‘classical’ thermal conduction. Without additional information about the geometry of the observed loops, it is impossible to make definite conclusions on the viewing angle. However, we expect the actual detection lengths to be of the same order of magnitude as the observed detection lengths. Including loop curvature, an offset of the loop centre from the base of the corona and inclination with respect to the vertical will result in a further decrease of the perturbations amplitudes, as these factors reduce the effect of gravity along the loop ([Tsiklauri & Nakariakov 2001](#)).

Using a two-dimensional model with a transversal density profile, [De Moortel *et al.* \(2004b\)](#) studied the coupling of slow and fast MHD waves in a coronal (i.e. plasma beta less than 1) environment. It was found that the coupling to the fast wave is an inefficient way to extract energy from the driven slow wave and hence is unlikely to make a large contribution to the rapid damping of the observed waves. This is in agreement with the results of [Rosenthal *et al.* \(2002\)](#) and [Bogdan *et al.* \(2003\)](#) who numerically demonstrated that the coupling between slow and fast modes is only effective where the sound and Alfvén speed are comparable in magnitude, i.e. where the plasma beta approaches unity. The phase mixing of the slow waves due to the transversal density inhomogeneity does cause damping of the oscillation amplitude, but is again too weak to explain the observed damping rates.

5. Coronal seismology

(a) *Coupling of the solar atmosphere*

Unlike most of the other observed examples of waves and oscillations in the solar corona, the propagating slow waves do not appear to be induced by a nearby impulsive event but are likely to be driven by oscillations in the underlying atmospheric layers. This provides an opportunity to investigate the coupling between and the properties of the different atmospheric layers. Given that, ultimately, the energy needed to maintain the million degree corona has to come from the solar convection zone (which is situated just below the surface), understanding the connectivity of the solar atmosphere is key to our understanding of the corona. There is a large number of reports on oscillations in the photosphere, chromosphere and transition region, in a large number of different structures (sunspots, coronal holes, the chromospheric network and internetwork regions, etc.). In this review, we will only highlight some of the more recent studies, that have concentrated on the (simultaneous) detection of oscillations in different parts of the solar atmosphere and that have demonstrated how the observed oscillations can contribute to our understanding of the local plasma structure and dynamics.

For example, [Wikstøl *et al.* \(2000\)](#) analysed solar ultraviolet measurements of emitted radiation (SUMER)/SOHO time-series and found evidence of small-amplitude oscillations, which they interpret as upward propagating

waves in the upper chromosphere, driving an oscillation in the transition region. Judge *et al.* (2001) study the behaviour of oscillations in the photosphere, chromosphere and transition region. They show that a large part of the chromospheric dynamics is dominated by the photospheric p -modes, with the coherence becoming less clear in the transition region, possibly caused by the interaction between the waves and the magnetic field. Investigating the dynamics of two different active regions from a comparison between the oscillatory power in the photosphere and chromosphere, Muglach (2003) also suggests that some of the observed features can be explained by the difference in the magnetic field topology. Further evidence for this interaction between oscillations and the magnetic field is presented by McIntosh *et al.* (2003), inferred from a strong correlation between the topography of the chromosphere and the behaviour of observed oscillations. Concentrating on network bright points, McAteer *et al.* (2003) detected propagating oscillations in the lower and upper chromosphere and possible evidence for mode coupling between kink- and sausage-modes waves.

As was shown by De Moortel *et al.* (2002c), the periodicity of the propagating oscillations appeared to be strongly correlated to the location of the loops: loops above sunspots showed oscillations of the order of 3 min, whereas the other loops had periodicities of about 5 min. It is well known that 3 min oscillations occur in the umbra of sunspots and several authors have provided observational evidence that these oscillations propagate up along the magnetic field lines, through the chromosphere and transition region, into the lower corona. For example, O'Shea *et al.* (2002) detected oscillations, which are likely to be propagating slow waves, in a sunspot umbra, from the temperature minimum to the coronal temperature of $\log T=6.4$. Similarly, Brynildsen *et al.* (2002) reported a 3 min period oscillation above a sunspot umbra and found that the oscillation amplitudes increase with increasing temperature, reaching a maximum at about $1-2 \times 10^5$ K and then decreasing again in the higher temperature lines. As demonstrated by Rendtel *et al.* (2003), the analysis of observed oscillations in the chromosphere and transition region above sunspots has the potential to reveal rapidly changing conditions in this part of the solar atmosphere. More recently, Marsh & Walsh (2004) found 3 min oscillations observed in He I and O V, above a sunspot umbra, which are then seen to propagate along active region loops observed by TRACE.

As described above, several authors have provided evidence that the observed oscillations can provide a powerful tool to probe the structure, the behaviour and the coupling between the various (lower) layers of the solar atmosphere. Additionally, for the 3 min oscillations, the coupling to the corona is also well established in the literature. The situation for the 5 min oscillations is, both theoretically and observationally, far less clear. The 5 min, global oscillations of the solar surface have been studied in great detail and there is sufficient observational evidence for 5 min oscillations in a variety of coronal structures. However, reports of observations of the propagation of 5 min oscillations from the surface into the corona are limited. Baudin *et al.* (1996) report upwardly propagating, 5 min, magnetoacoustic waves in the solar chromosphere. Similarly, Marsh *et al.* (2003) found evidence for ~ 300 s oscillations at chromospheric (He I), transition region (O V) and coronal (Mg IX) temperatures. The observed

oscillations are co-spatial and co-temporal with upwardly propagating, 5 min, oscillations observed by TRACE in a coronal loop.

Studying active region moss (bright and dynamic, transition region emission, situated above active region plage and at the base of hot coronal loops), De Pontieu *et al.* (2003a) found evidence for small scale correlations between chromospheric and transition region emission in active regions. Continuing the analysis, De Pontieu *et al.* (2003b) show that moss exhibits periodicities of the order of 200–600 s, typically in cycles of 4–7 periods. The oscillations are usually detected at the edges of active regions and are directly associated with (upper) chromospheric oscillations (spicules). There is also some evidence of a (possibly nonlinear) correlation with the photospheric p -modes. Using numerical modelling that combines all the observed evidence, De Pontieu *et al.* (2004) show that the observed periodicity of spicules and hence, moss, can be explained by p -modes travelling from the photosphere along inclined field lines. Extending this study into the corona, De Pontieu *et al.* (2005) show that the quasi-periodic shocks that drive the spicules travel upward into the corona and thus might be responsible for the propagating, 5 min oscillations observed in coronal loops. This model provides a natural explanation for the many similarities between moss and longitudinal loop oscillations and despite the lack of direct observations, it could provide the elusive link between the 5 min oscillations observed at the solar surface and in the corona.

(i) *Sub-resolution fine-structure of coronal loops*

Using EIT/SOHO and TRACE, Robbrecht *et al.* (2001) observed propagating, 5 min oscillations in a fan of coronal loops in both the 195 Å (*ca* 1.5 MK) and the 171 Å (*ca* 1 MK) passbands. They find that the oscillations propagate with different speeds, which, given that the sound speed depends on the temperature, is in agreement with the interpretation of the observed oscillations as propagating, slow MHD waves. A similar result was obtained by King *et al.* (2003) using both the TRACE 195 and 171 Å passbands. The improved resolution of the TRACE observations allowed the additional study of the correlation between the two passbands. This was found to be relatively high near the loop footpoints but tends to decrease as the perturbations travel along the loops. This loss of coherence could be due to the different propagation speeds, corresponding to different temperatures, and hence could be an indication of a multi-strand (sub-resolution) loop structure (Nakariakov & Verwichte 2005). Berghmans *et al.* (2001) found evidence of propagating slow waves in a much hotter coronal loop ($T \approx 5.1$ K), again observed as intensity perturbations travelling at the local sound speed (*ca* 310 km s⁻¹). Using observed oscillations to infer the unresolved fine-structure of coronal loops is a promising possibility, certainly deserving further development.

Additionally, it was pointed out by Kelly & Nakariakov (2004) that the observed propagating slow waves, when interpreted as magnetoacoustic autowaves, could be used to determine the location of the heat deposition in coronal loops. The exact form of the heating function along coronal loops is still uncertain and recently has been the issue of much debate (see Walsh & Ireland 2003 for a review).

6. Conclusions

In this paper, we have given an overview of the properties of propagating intensity perturbations, detected in high cadence extreme ultraviolet observations of coronal loops. The oscillations appear to be a regularly occurring feature in loops situated in active region plage, where a 5 min periodicity is most often found, and sunspots, where 3 min periods prevail. The observed oscillations are interpreted as propagating slow magnetoacoustic waves and, using a 1D model, the very rapid observed damping can be explained in terms of ‘classical’ thermal conduction, without the need to invoke an anomalously large conduction coefficient. The quasi-periodic disturbances are most likely driven by underlying solar oscillations, providing an opportunity to study the coupling and coherence of the solar atmosphere. Numerical simulations show that the 5 min surface oscillations, travelling along inclined field lines, could be responsible for the observed periodicity. Finally, the robustness of wavelet analysis was briefly discussed, highlighting the need for a careful interpretation of the results of wavelet analysis.

The author acknowledges support of a Royal Society University Research Fellowship.

References

- Baudin, F., Bocchialini, K. & Koutchmy, S. 1996 *Astron. Astrophys.* **314**, L9.
- Berghmans, D. & Clette, F. 1999 *Sol. Phys.* **186**, 207. (doi:10.1023/A:1005189508371)
- Berghmans, D., McKenzie, D. & Clette, F. 2001 *Astron. Astrophys.* **369**, 291.
- Bogdan, T. J. *et al.* 2003 *Astrophys. J.* **599**, 626. (doi:10.1086/378512)
- Brynildsen, N., Maltby, P., Fredvik, T. & Kjeldseth-Moe, O. 2002 *Sol. Phys.* **207**, 259. (doi:10.1023/A:1016238317702)
- DeForest, C. E. & Gurman, J. B. 1998 *Astrophys. J.* **501**, L217. (doi:10.1086/311460)
- De Moortel, I. 2005 *Phil. Trans. R. Soc. A* **363**, 2743.
- De Moortel, I. & Hood, A. W. 2003 *Astron. Astrophys.* **408**, 755. (doi:10.1051/0004-6361:20030984)
- De Moortel, I. & Hood, A. W. 2004 *Astron. Astrophys.* **415**, 705. (doi:10.1051/0004-6361:20034233)
- De Moortel, I., Ireland, J. & Walsh, R. W. 2000 *Astron. Astrophys.* **355**, L23.
- De Moortel, I., Ireland, J., Walsh, R. W. & Hood, A. W. 2002a *Sol. Phys.* **209**, 61. (doi:10.1023/A:1020956421063)
- De Moortel, I., Ireland, J., Hood, A. W. & Walsh, R. W. 2002b *Sol. Phys.* **209**, 89. (doi:10.1023/A:1020960505133)
- De Moortel, I., Ireland, J., Hood, A. W. & Walsh, R. W. 2002c *Astron. Astrophys.* **387**, L13. (doi:10.1051/0004-6361:20020436)
- De Moortel, I., Munday, S. A. & Hood, A. W. 2004a *Sol. Phys.* **222**, 203. (doi:10.1023/B:SOLA.0000043578.01201.2d)
- De Moortel, I., Hood, A. W., Gerrard, C. L. & Brooks, S. J. 2004b *Astron. Astrophys.* **425**, 741. (doi:10.1051/0004-6361:20040391)
- De Pontieu, B., Tarbell, T. & Erdélyi, R. 2003a *Astrophys. J.* **590**, 502. (doi:10.1086/374928)
- De Pontieu, B., Erdélyi, R. & de Wijn, A. G. 2003b *Astrophys. J.* **595**, L63. (doi:10.1086/378843)
- De Pontieu, B., Erdélyi, R. & James, S. P. 2004 *Nature* **430**, 536. (doi:10.1038/nature02749)
- De Pontieu, B., Erdélyi, R. & De Moortel, I. 2005 *Astrophys. J.* **624**, L61.
- Judge, P. G., Tarbell, T. D. & Wilhelm, K. 2001 *Astrophys. J.* **554**, 424. (doi:10.1086/321383)
- Kelly, A. & Nakariakov, V. M. 2004 *ESA SP* **547**, 483.
- King, D. B., Nakariakov, V. M., Deluca, E. E., Golub, L. & McClements, K. G. 2003 *Astron. Astrophys.* **404**, L1. (doi:10.1051/0004-6361:20030763)

- Klimchuk, J. A., Tanner, S. E. M. & De Moortel, I. 2004 *Astrophys. J.* **616**, 1232. (doi:10.1086/425122)
- Marsh, M. S., Walsh, R. W., De Moortel, I. & Ireland, J. 2003 *Astron. Astrophys.* **404**, L37. (doi:10.1051/0004-6361:20030709)
- Marsh, M. S. & Walsh, R. W. 2004 *ESA SP* **547**, 108.
- McAteer, R. J. T., Gallagher, P. T., Williams, D. R., Mathioudakis, M., Bloomfield, D. S., Phillips, K. J. H. & Keenan, F. P. 2003 *Astrophys. J.* **587**, 806. (doi:10.1086/368304)
- McIntosh, S. W., Fleck, B. & Judge, P. G. 2003 *Astron. Astrophys.* **405**, 769. (doi:10.1051/0004-6361:20030627)
- Muglach, K. 2003 *Astron. Astrophys.* **401**, 685. (doi:10.1051/0004-6361:20021901)
- Nakariakov, V. M. & Verwichte, E. 2005 *Liv. Rev. Sol. Phys.* **2**, 3.
- Nakariakov, V. M., Verwichte, E., Berghmans, D. & Robbrecht, E. 2000 *Astron. Astrophys.* **362**, 1151.
- Nightingale, R. W., Aschwanden, M. J. & Hurlburt, N. E. 1999 *Sol. Phys.* **190**, 249. (doi:10.1023/A:1005211618498)
- Ofman, L. & Wang, T. J. 2002 *Astrophys. J.* **580**, L85. (doi:10.1086/345548)
- Ofman, L., Romoli, M., Poletto, G., Noci, C. & Kohl, J. L. 1997 *Astrophys. J.* **491**, L111. (doi:10.1086/311067)
- Ofman, L., Nakariakov, V. M. & DeForest, C. E. 1999 *Astrophys. J.* **514**, 441. (doi:10.1086/306944)
- Ofman, L., Romoli, M., Poletto, G., Noci, C. & Kohl, J. L. 2000a *Astrophys. J.* **529**, 592. (doi:10.1086/308252)
- Ofman, L., Nakariakov, V. M. & Seghal, N. 2000b *Astrophys. J.* **533**, 1071. (doi:10.1086/308691)
- O'Shea, E., Muglach, K. & Fleck, B. 2002 *Astron. Astrophys.* **387**, 642. (doi:10.1051/0004-6361:20020375)
- Rendtel, J., Staude, J. & Curdt, W. 2003 *Astron. Astrophys.* **410**, 315. (doi:10.1051/0004-6361:20031189)
- Roberts, B., Edwin, P. M. & Benz, A. O. 1984 *Astrophys. J.* **279**, 857. (doi:10.1086/161956)
- Robbrecht, E., Verwichte, E., Berghmans, D., Hochedez, J. F., Poedts, S. & Nakariakov, V. M. 2001 *Astron. Astrophys.* **370**, 591. (doi:10.1051/0004-6361:20010226)
- Rosenthal, C. S., Bogdan, T. J., Carlsson, M., Dorch, S. B. F., Hansteen, V., McIntosh, S. W., McMurry, A., Nordlund, Å. & Stein, R. F. 2002 *Astrophys. J.* **564**, 508. (doi:10.1086/324214)
- Schrijver, C. J. *et al.* 1999 *Sol. Phys.* **187**, 261. (doi:10.1023/A:1005194519642)
- Torrence, C. & Compo, G. P. 1998 *Bull. Am. Meteorol. Soc.* **79**, 61. (doi:10.1175/1520-0477(1998)079<0061:APGTWA>2.0.CO;2)
- Tsiklauri, D. & Nakariakov, V. M. 2001 *Astron. Astrophys.* **379**, 1106. (doi:10.1051/0004-6361:20011378)
- Walsh, R. W. & Ireland, J. 2003 *Astron. Astrophys. Rev.* **12**, 1. (doi:10.1007/s00159-003-0021-9)
- Wikstøl, Ø., Hansteen, V. H., Carlsson, M. & Judge, P. G. 2000 *Astrophys. J.* **531**, 1150.

Discussion

P. S. CALLY (*Department of Mathematics and Statistics, Monash University, Clayton, Victoria, Australia*). You found in 1D that thermal conduction is crucial. Shouldn't it therefore be included in the 2D model?

I. DE MOORTELE. The aim of the 2D model was to investigate the contribution of mode coupling between the slow and fast MHD modes and phasemixing of the slow mode to the damping of the (driven) slow modes. In order to isolate just these effects, thermal conduction was excluded from the 2D model. Of course, in a next stage, thermal contribution could be included again in the model.

I. BALLAI (*Space and Atmosphere Research Centre, Department of Applied Mathematics, University of Sheffield, UK*) Can the speaker estimate how large

the wavelengths of the observed slow waves are compared with the transversal size of the loops?

I. DE MOORTELE. A rough estimate of the wavelength can be obtained by taking a period of 300 s and a propagation speed of about 150 km s^{-1} . This results in a wavelength of about 45 Mm. The transversal size of the loop segments in which the oscillations are observed is in the range of 5–15 Mm.